Nanoscale thermal stabilization via permutational premelting

Francesc Viñes,[1] Javier Carrasco,[2] and Stefan T. Bromley[1,3,*]

[1]*Departament de Química Física and Institut de Química Teòrica i Computacional, Universitat de Barcelona, E-08028 Barcelona, Spain*

[2]*Instituto de Catálisis y Petroleoquímica, CSIC, Marie Curie 2, E-28049 Madrid, Spain*

[3]*Institució Catalana de Recerca i Estudis Avançats (ICREA), 08010 Barcelona, Spain*

(Received 18 November 2011; published 14 May 2012)

Anomalous higher-than-bulk melting in some metal clusters has been previously ascribed to particularly compact cluster structures and emergent covalent bonding at small sizes. Using both classical and *ab initio* molecular dynamics incorporating realistic interacting atomic environments, we show a MgO cluster which, although structurally flexible and with bulklike ionic bonding, melts at a higher temperature than rock salt MgO. We propose that this unexpectedly high thermal stability is due to the premelted dynamics of a bi-isomeric fluxional state allowing facile permutation of ion positions, raising the configurational entropy and lowering the free energy. We argue that this entropic stabilizing effect could also occur in other (nano)systems which allow for atomic permutations with relatively little structural change.

DOI: 10.1103/PhysRevB.85.195425 PACS number(s): 61.46.Bc, 36.40.Ei, 36.40.Qv, 65.80.−g

I. INTRODUCTION

Understanding the detailed mechanisms of crystalline solid melting remains a fundamental challenge to experimentalists and theorists alike. Upon heating, but below the melting temperature ($T_{\mathrm{melt[bulk]}}$), a bulk solid may transform into other stable crystal phases and start to exhibit an increase in local atomic disorder at surfaces[1] and defects.[2] These so-called premelting effects can have significant large-scale environmental and geological consequences.[3,4] Premelting is strongly influenced by reduction in scale and dimensionality,[5] playing a fundamental role in the thermodynamics of nanoscale condensed matter. Endeavors to understand melting at the microscopic scale have largely focused on atomic nanoclusters, with breakthroughs coming from cluster beam experiments and computational simulations.[6–8] The latter, uniquely providing detailed atomic scale information, has highlighted premelting phenomena in nanoclusters analogous to that found in the bulk (e.g., surface[9] and stepwise[10] premelting). Contrary to typically sharp bulk melting transitions, seminal computational simulations of small inert gas clusters showed that nanoclusters can exist in phase coexistence states, fluctuating between solidlike and liquidlike phases over a premelted temperature range.[11]

Previous simulation studies have mainly concentrated on closed-packed monoelemental clusters (e.g., pure metals and rare gases) rather than clusters of compound materials. Theoretical studies of the finite temperature behavior of clusters of the latter class have been almost solely dedicated to alkali halide systems.[12–18] Such clusters with over ∼60 ions tend to display extended periods in either ordered or disordered phases, with only occasional jumps in between,[12,16,17] whereas simulations of smaller clusters have revealed a variety of dynamic phase coexistence states[13,15,18] during premelting, where various isomers are sampled. Such works, and other studies on small metal clusters,[19,20] have been instrumental in providing uniquely detailed insights into cluster melting.

Particularly interesting from a bulk melting perspective are the anomalous observations of some metal clusters with $T_{\mathrm{melt[cluster]}} > T_{\mathrm{melt[bulk]}}$.[21] To rationalize such experimental findings, proposed explanations have focused on the increased strength and stiffness of emergent covalent bonds in these particular metal clusters compared to the bulk.[8,22,23] Conversely, we demonstrate higher-than-bulk melting in highly ionic nonmetallic nanoclusters, which we ascribe to a premelted dynamical state with associated high configurational entropy. Specifically, by means of molecular dynamics (MD) calculations we center our study on a cluster of the archetypal ionic insulator MgO for which we find a premelted state allowing facile oscillations between two distinct isomers, leading to rapid permutations involving all ions. Although permutationally fluidlike, the cluster's extremely limited structural isomerization possibilities clearly demark the system as not fully melted. We denote this peculiar type of intermediate microscopic state as being fully (i.e., involving all of a cluster's ions/atoms) permutationally premelted. Comparing with bulk calculations, we find that the fully permutationally premelted state persists until it isomerically melts with $T_{\mathrm{melt[cluster]}} > T_{\mathrm{melt[bulk]}}$. Fully permutationally premelted systems may possess a high degree of atomic disorder (i.e., configurational entropy, S_{conf}) while retaining a relatively solidlike state. We propose that the associated $(-T\Delta S)$ free energy decrease rationalizes the significant increase in $T_{\mathrm{melt[cluster]}}$ and that full permutational premelting can be at least as important as structural rigidity and chemical bonding in determining the thermal stability of nanoclusters.

II. METHODOLOGY

We focus our study on a small cluster of the prototypical ionic oxide MgO with composition Mg_6O_6 using isoenergetic MD simulations. As confirmed previously, the cluster's two lowest energy isomers are: a drumlike hexagonal form (ground state) and a cubic form[24–27] (see Fig. 1). We note also that the Mg_6O_6 cluster is also the smallest of the series of "magic" MgO clusters with the general formula $(MgO)_{3n}$ (n = 2–10) as abundantly found in cationic cluster beam experiments.[28,29] We employed two types of MD calculations: (i) classical, with interionic potentials (IPMD), and (ii) *ab initio* (AIMD), using density functional (DF) theory, in order

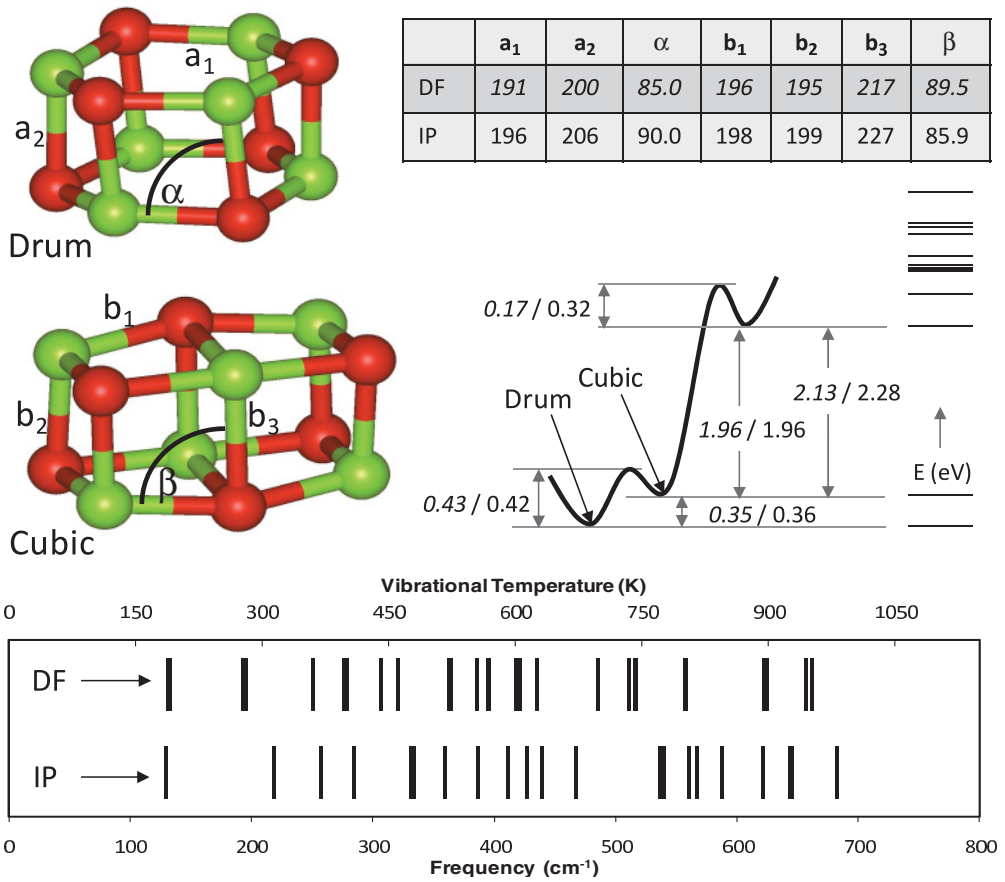

	a_1	a_2	α	b_1	b_2	b_3	β
DF	*191*	*200*	*85.0*	*196*	*195*	*217*	*89.5*
IP	196	206	90.0	198	199	227	85.9

FIG. 1. (Color online) Geometric (picometers [pm] and degrees), energetic (computed by DF/IP, eV), and vibrational properties (Mg_6O_6 drum) of Mg_6O_6 clusters (Mg-green/light gray, O-red/gray).

to investigate the finite temperature behavior of Mg_6O_6 as a general model of ionic A_6B_6 systems. Born-Oppenheimer AIMD (prethermalized 50 ps runs, 75 ps near $T_{\text{melt[cluster]}}$) and IPMD (prethermalized 10 ns runs) simulations were carried out within the microcanonical ensemble. For a sufficiently accurate time evolution (taken to be when the total energy drift was <0.001 eV/ps) a MD time step of 1 fs was employed throughout. The MD simulations employed a very dilute bath of 10 He atoms, with initial random velocities appropriate for the simulation temperature, in order to address a series of issues. Firstly, He is frequently used in cluster beam experiments as an inert thermalizing agent and thus is a realistic addition to the simulations. Secondly, the occasional collisions of He with the cluster helps ensure against known spurious effects of nonergodic behavior, known to be a problem for systems prepared using the Berendsen thermostat,[30,31] as used herein, and for a number of isolated simple dynamical systems (e.g., ideal coupled oscillators). We found that the calculations using a He bath gave more reliable averages for obtaining data points for the calorific curve in single relatively short MD runs without needing to average over separate randomly initialized runs. This feature makes it particularly useful for reducing unnecessary computational costs in AIMD simulations. We note that He-cluster collisions (typically one per ps with three-particle collisions hardly ever witnessed, thus not contributing any significant net pressure) do not induce permutational premelting, nor do they affect $T_{\text{melt[cluster]}}$. To highlight the latter, we show in Fig. 2 the calorific curve (lower in energy due to the lacking He kinetic energy) obtained from an IPMD simulation of a nonrotating Mg_6O_6 cluster with a fixed center of mass, showing the same $T_{\text{melt[cluster]}}$ as in the case with the He bath. The IPMD simulations used MgO-He and He-He repulsive interaction potentials based on those in Refs. 32 and 33, respectively. All DF calculations were carried out at the $\mathbf{\Gamma}$ point using the VASP code[34] and the PW91 functional,[35] with inner cores described by the projector augmented wave method[36] and a plane-wave cutoff of 415 eV. Transition states between minima were located with the climbing-image nudged-elastic-band (CI-NEB) algorithm.[37] Harmonic vibrational frequency analysis showed that all transition states had only one imaginary frequency and all minima had only positive frequencies. The IPs used a repulsive Born interaction term between Mg and O ions [i.e., $A_{ij}\exp(-r_{ij}/\rho_{ij})$ with $A_{MgO} = 1226.0$ eV and $\rho_{MgO} = 0.301$ Å] with electrostatic interactions provided by partial ionic charges of $\pm 1.75\ e$, providing a good match with DF calculations of: (i) structure, (ii) minima and transition state energies, and (iii) vibrational frequencies (see Fig. 1). We carried out both classical and DF calculations employing periodic boundary conditions with a cubic box ($16 \times 16 \times 16$ Å^3) large enough to ensure that repeated image interactions were negligible. Relative root mean square interionic distance fluctuations were calculated using a cluster-adapted Lindemann index (δ); see, e.g., Ref. 11.

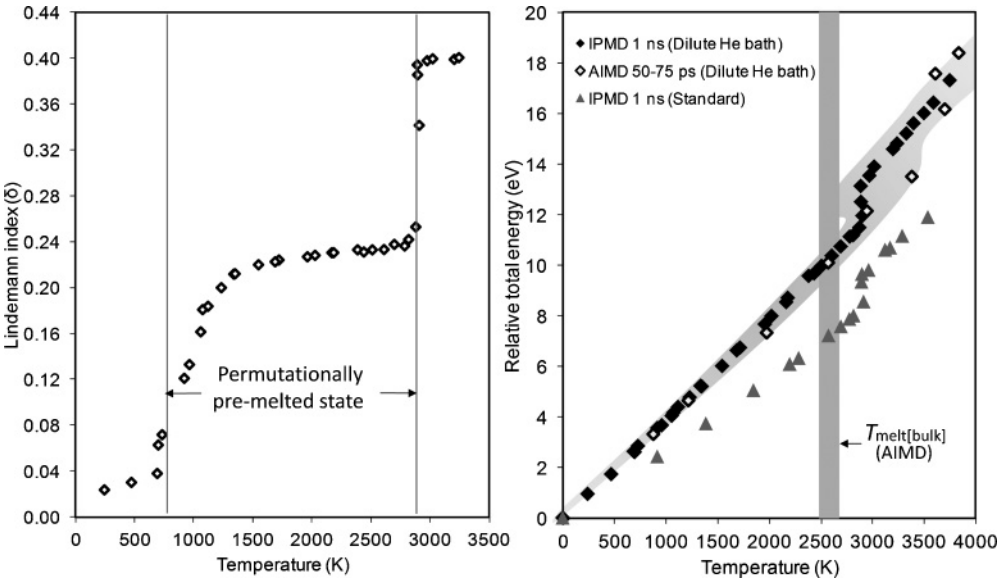

FIG. 2. Temperature dependence of (i) Lindemann index (δ) for IPMD runs (left), (ii) relative total energy with respect to Mg_6O_6 drum for IPMD and AIMD runs (right). The vertical gray bar shows the $T_{\text{melt[bulk]}}$ range calculated in Ref. 40. The light grey shaded region indicates the temperature uncertainty in the AIMD data.

III. RESULTS AND DISCUSSION

Using energy barriers in Fig. 1 we can estimate the drum $\rightarrow$ cubic transition temperature. Assuming ergodic conditions we can use the equipartition theorem to estimate the minimum temperature T at which the barrier crossing is possible (i.e., $Ak_BT = \langle E_{KE}\rangle$, where A is the number of vibrational degrees of freedom, k_B is the Boltzmann constant, and $\langle E_{KE}\rangle$ is the average total vibrational kinetic energy). Equating $\langle E_{KE}\rangle$ to the barrier height gives $T \sim 330$ K for both IP and DF calculations. Generally, other competing accessible modes may not facilitate drum $\leftrightarrow$ cubic transformations, hindering the reversible barrier crossing by taking up their share of $\langle E_{KE}\rangle$ (thus raising temperatures for likely barrier crossings). The calculated IP and DF vibrational spectra are very similar and consistently give vibrational temperatures ranging between 150 and 1000 K (see Fig. 1). The drum $\leftrightarrow$ cubic barrier crossing is associated with the lowest doubly degenerate mode of the drum cluster with a vibrational temperature of $\sim$190 K for both sets of calculations. The mode is a breathing displacement of ions parallel to the hexagonal planes of the drum cluster compressing the drum along its widest diameter to become more cubic and vice versa. We observe its first effect in the IPMD calculations at temperatures $\geqslant$650 K, where it assists the drum $\leftrightarrow$ cubic isomer interchange frequently enough to significantly affect the time-averaged atomic disorder in the cluster as measured by δ (see Fig. 2).

The initial transition from a weakly thermally excited drum to a drum $\leftrightarrow$ cubic premelted phase has no calorific curve counterpart, confirming its non-fully-melted status. This low-frequency breathing mode and the associated fluxional premelted state, sampling only drum and cubic isomers, dominates the dynamics and persists up to $\sim$2900 K (>3300 K) in the IPMD (AIMD) simulations. Considering this isomerization as an opening and closing of the structure with no interchange of ions the state can be viewed as a "hot solid."[15] However, we also find this topological isomerization can lead to arbitrary ion permutations due to the nonuniqueness of the drum $\leftrightarrow$ cubic opening and closing dynamics. In Fig. 3 we show how a single ion can migrate to all symmetrically inequivalent positions in either drum or cubic isomers via a maximum of four drum $\leftrightarrow$ cubic steps. As this permutationally premelted state allows for almost complete time-averaged atomic disorder, while only accessing two isomers, it is unclear how close it is to being fully melted. To discriminate premelted cluster states from the truly melted liquid state, Rose and Berry[18] proposed that two necessary dynamic criteria should be satisfied for the latter: The time scale characterizing the interconversion between different cluster isomers, T_{int}, must be (i) within a factor of $\sim 10^2$ times larger than that of the time scale of cluster vibrations, T_{vib}, and (ii) not much shorter than the time scale for accessing different permutational isomers, T_{perm}. In the permutationally premelted M_6O_6 cluster the freedom to follow different isomerization pathways opens up the possibility for a rapid atom interchange on the time scale of the interwell drum $\leftrightarrow$ cubic dynamics (i.e., $T_{\text{int}} \approx T_{\text{perm}}$). For our calculations $T_{\text{int}} \approx 1$ ps and $T_{\text{perm}} \approx 2$ ps. Considering that drum $\leftrightarrow$ cubic transformation comes about via a low-frequency vibrational mode, T_{int} is also within a factor or 10^2 of T_{vib}. Therefore, only considering drum and cubic isomers, the M_6O_6 permutationally premelted state can, to a large extent, be regarded as being melted.

Due to the magnitude of T_{perm} and the high number of permutational possibilities, the computationally demanding AIMD simulations are not long enough to obtain reliable averages of configurational disorder and thus δ is only given for the IPMD calculations. Nevertheless, for the calorific curve, as permutational isomers have the same energy, the averages are insensitive to ion interchanges, making sampling much more efficient. The AIMD production run lengths were found to give highly reproducible kinetic energy averages for constructing the calorific data for the premelted regime in

line with the 1 ns IPMD runs. Near the energy of the melting transition, although longer (75 ps) AIMD runs were performed, the discrepancy with the IPMD predicted temperatures is noticeably larger for one AIMD data point at 3380 K. Based on over 200 independent 50 ps IPMD runs with a range of starting conditions we have calculated the inherent averaging error of relatively short MD runs with respect to the fully converged 1 ns runs. This analysis (shaded region in Fig. 2) confirms that the maximum discrepancy is, unsurprisingly, most likely around the melting transition, with corresponding maximum temperature errors of $\pm 14\%$. The IPMD data shows a premelted linear increase in energy with temperature until a $\sim$1.7 eV vertical step at $\sim$2900 K, indicating a melting transition, afterwards following a y-shifted linear increase. Thus the AIMD data are fully consistent with the IPMD data, taking the AIMD data point at 3380 K to be a maximally ($\sim$14%) overheated state. A $T_{\mathrm{melt[cluster]}}$ of 2900 K is also indicated in the IPMD simulations via δ (see Fig. 2), identified with a configurational space opening where cluster isomers other than the drum and cubic are sampled (see energies of higher-lying isomers in Fig. 1). Once the barrier to the next isomer above the cubic isomer is breached all other higher-energy isomer minima are separated only $\sim$0.3 eV (see Fig. 1) and thus full melting via multiple isomerization is facilitated. We note that since the IPs used in the IPMD runs were specifically parametrized to the small size regime of the Mg_6O_6 cluster IPMD simulations, and thus most suitable for evaluating $T_{\mathrm{melt[cluster]}}$, they are not suitable for bulk MgO calculations, and totally inappropriate for obtaining a reliable value of $T_{\mathrm{melt[bulk]}}$. Although efforts to design ionic IPs that are transferable to different length scales and physical conditions have been made,[38] it is doubtful that reliable results would be obtained by any IP in the extreme comparison of the melting of very small clusters and the infinite bulk. Other IPMD simulations using similar IPs to those used herein found $T_{\mathrm{melt[cluster]}} \approx 2000$ K for $(MgO)_{3n}$ clusters ($n = 6$–8).[39] Using these IP parameters we also find a $T_{\mathrm{melt[cluster]}}$ for Mg_6O_6 of $\sim$2900 K confirming our IPMD results. Alternatively, for comparing our cluster melting results with the bulk, one may employ inherently size-transferable AIMD calculations for the bulk. Using an almost identical DF setup to that used herein, the zero pressure $T_{\mathrm{melt[bulk]}}$ of rock salt MgO was calculated to be 2575 $\pm$ 100 K,[40] giving at most a 225 K lower value than we predict for $T_{\mathrm{melt[cluster]}}$. Interestingly, this bulk value may even be susceptible to a small corrective upshift of $\sim$3% due to premelting effects identified in an IPMD study.[41] Even additionally considering this possible upshift, our data still predict that the Mg_6O_6 cluster melts at a significantly higher temperature (180–350 K) than that of the bulk.

Although small clusters have fewer bonds per atom, they are often shorter and stiffer than in the bulk, which has been proposed as an explanation of the increased thermal stability of some clusters.[23] Our calculations of a range of $(MgO)_{3n}$ ground state clusters reveal them to have shorter Mg-O bonds (by 0.1–0.2 Å) than bulk rock salt MgO. As noted above, Mg_6O_6 melts at $\sim$900 K above other similar sized clusters which also have similar bond contractions ruling out bond length considerations as the probable reason for its high thermal stability. Shortened bonds may also display increased covalency which has been proposed to be the main cause of elevated $T_{\mathrm{melt[cluster]}}$ in some metal clusters.[22,42] Bader-partitioned atomic charges[43] in bulk rock salt MgO and Mg_6O_6 drum and cubic clusters are found to have the same value ($\pm 1.7\,e$). Analysis of the electron localization function[44] (ELF) further confirms the highly ionic status of bulk and clusters, with the first indication of any electron pairs between ions (i.e., covalency) occurring at the low values of 0.06 and 0.11, respectively. Without convincing evidence of bulk vs cluster bonding differences, we turn our attention to premelting dynamical effects as being responsible for the higher-than-bulk $T_{\mathrm{melt[cluster]}}$ in Mg_6O_6.

For ionic Mg_6O_6 we propose that the thermal stability increase is mainly due to fully permutational premelting, lowering the free energy due to a significant increase in S_{conf}. To understand how surface premelting influences $T_{\mathrm{melt[cluster]}}$ in metal clusters it has been shown to be important to take into account S_{conf}.[45] Equating the free energies of the premelted and fully melted cluster at $T_{\mathrm{melt[cluster]}}$ gives $T_{\mathrm{melt[cluster]}} = (E_{\mathrm{melted[cluster]}} - E_{\mathrm{premelted[cluster]}})/(S_{\mathrm{melted[cluster]}} - S_{\mathrm{premelted[cluster]}}) = \Delta E/\Delta S$, where E and S are total cluster energies and entropies, respectively. By definition $E_{\mathrm{melted[cluster]}}$ and $S_{\mathrm{melted[cluster]}}$ are unchanged by premelting and $E_{\mathrm{premelted[cluster]}}$ is also unchanged for permutational premelting. A liquidlike permutationally premelted cluster, however, has a relatively high configurational disorder (i.e., high $S_{\mathrm{premelted[cluster]}}$) making ΔS smaller which, in turn, raises $T_{\mathrm{melt[cluster]}}$. Alternatively stated, in fully permutationally premelted systems ΔS is not strongly correlated with ΔE, and does not act to strongly damp the energetic influence on $T_{\mathrm{melt[cluster]}}$ as it typically does.[46] Without the influence of ΔS it has been estimated that observed fluctuations in $T_{\mathrm{melt[cluster]}}$ would be three to four times higher than observed in experiment. Following the dynamics of the premelted fluxional state (Fig. 3), all six Mg cations and all six O anions can freely interchange their respective positions giving an increase in $S_{\mathrm{premelted[cluster]}}$ due to the S_{conf} of permutational premelting of $\ln[6!6!]k_{\mathrm{B}}$, or $13.9k_{\mathrm{B}}$ (where k_{B} is the Boltzmann constant). For the ΔE and $T_{\mathrm{melt[cluster]}}$ obtained from our MD simulations we can also evaluate ΔS. For a fixed $S_{\mathrm{melted[cluster]}}$ we can then estimate the significance of the S_{conf} increase due to permutational premelting on $S_{\mathrm{premelted[cluster]}}$, i.e., how much it reduces ΔS with respect to the case without full permutational premelting (a premelted bi-isomeric "hot solid" A_6B_6 cluster[15] with a S_{conf} of $\ln[2]k_{\mathrm{B}} = 0.7k_{\mathrm{B}}$. From this we confirm that S_{conf}, due to full permutational premelting, has a large effect (>1500 K) on $T_{\mathrm{melt[cluster]}}$, which contributes to it being $\sim$300 K higher than $T_{\mathrm{melt[bulk]}}$.

For previously studied metal cluster systems Al_{13}, Ga_{13},[47] and Sn_{10},[42] which also have $T_{\mathrm{melt[cluster]}} > T_{\mathrm{melt[bulk]}}$, the ascribed reason for this phenomenon was their particular structures and the emergence of covalent bonding. Although for Sn_{10} dynamical permutations were noted as important in Ref. 42, no explicit link between the resultant high configurational entropy and the calculated higher-than-bulk melting has been put forward for these systems. A careful reading of Refs. 47 and 42 reveals that Al_{13}, Ga_{13}, and Sn_{10} should all, in fact, exhibit full (or at least nearly full) permutational premelting. We note that higher S_{conf} values for these fully permutationally premelted metal clusters, Sn_{10} ($S_{\mathrm{conf}} = \ln[10!]k_{\mathrm{B}} = 15.1k_{\mathrm{B}}$) and Ga_{13} ($S_{\mathrm{conf}} = \ln[13!]k_{\mathrm{B}} =$

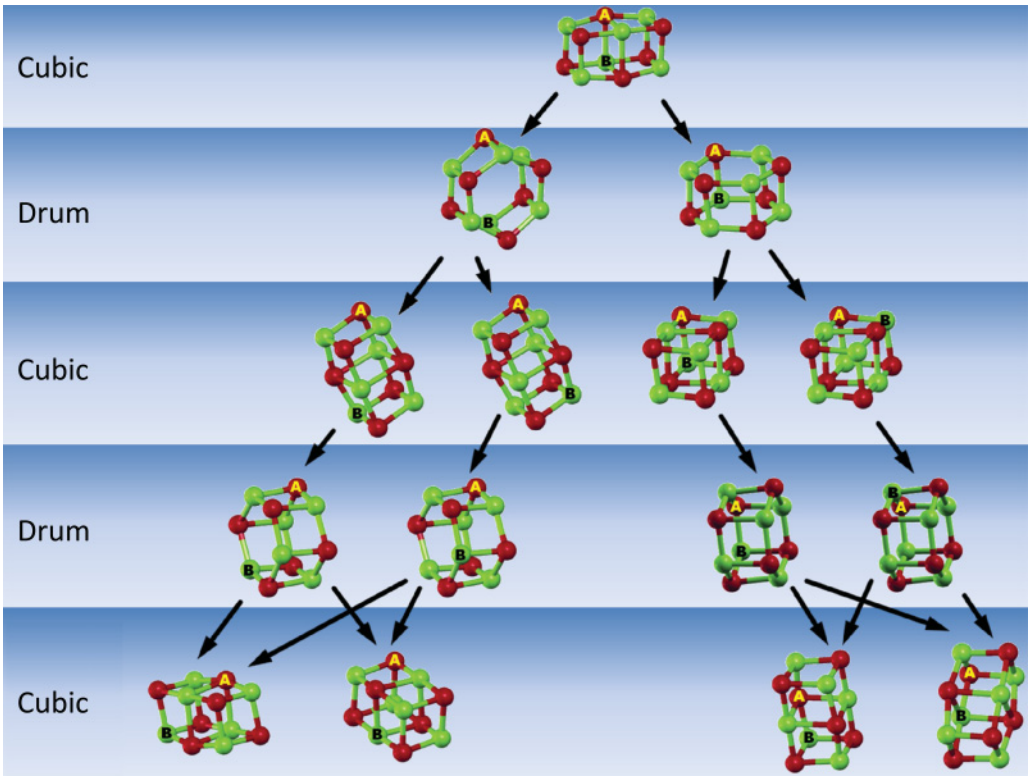

FIG. 3. (Color online) A (O) and B (Mg) ions can reach all symmetrically inequivalent relative positions within the drum ↔ cubic isomers through drum ↔ cubic transformations.

$22.6k_B$) coincide with relatively higher estimated increases of $T_{melt[cluster]}$ values above the corresponding $T_{melt[bulk]}$ values of ∼950 K and ∼890 K, respectively. We thus suggest that fully permutational premelting may also be an important factor in explaining the observation of $T_{melt[cluster]} > T_{melt[bulk]}$ in some metal cluster systems.

We believe that our proposed thermal stabilization via permutational premelting is likely to be general to many types of nanostructures and materials. For the opportunity for full permutation premelting to occur a system should allow for atom swapping via structural distortion. Although inhibited by dense bulk atomic packing, many nanosystems with the majority of their atoms near or at the surface could potentially provide the conditions for the effect to occur (e.g., fullerenelike clusters, nanotubes, thin sheets, layered materials, thin nanorods, nanoporous materials). Furthermore, to show that full permutational premelting via the drum ↔ cubic effect is not specific to only (neutral) Mg_6O_6, it is known that a wide range of binary AB materials have low-energy drum and cubic A_6B_6 isomers.[25,26,48] The DF-calculated barriers for the A_6B_6 drum ↔ cubic transformation for a range of materials and the cationic $(Mg_6O_6)^+$ system[49] are found to be similar to that for Mg_6O_6, and thus likely to give rise to a fully permutationally premelted state (see Fig. 4). Recently, a likely bi-isomeric mixture of drum-$(Mg_6O_6)^+$ and cubic-$(Mg_6O_6)^+$ has also been identified in cluster beams,[50] providing indirect evidence for drum ↔ cubic dynamics.

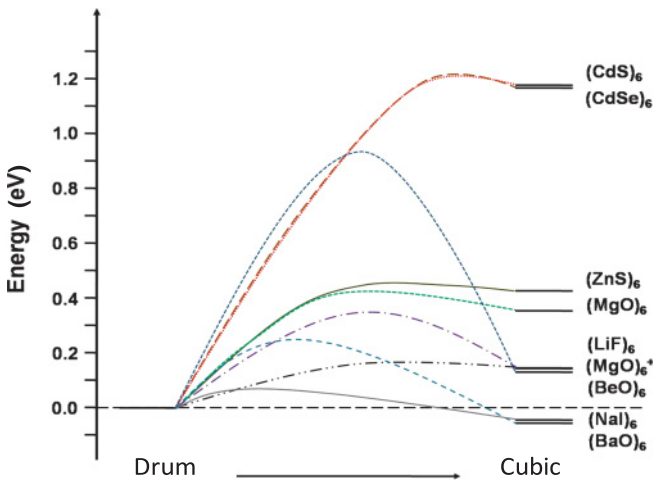

FIG. 4. (Color online) Relative energies and drum ↔ cubic barriers for various A_6B_6 clusters.

IV. CONCLUSIONS

Our investigation reveals that Mg_6O_6 clusters exhibit a fully permutationally premelted state which persists until full isomeric melting at higher-than-bulk melting temperatures. Considering the lack of any significant bulk-to-cluster bonding changes, we propose that the relatively high S_{conf} associated with permutational premelting is the main cause of the cluster's exceptional thermal stability. Comparing with the few other reports of metal clusters with higher-than-bulk melting, and via calculations on other A_6B_6 systems, we suggest that thermal stabilization through fully permutational premelting may be a widespread phenomenon. In addition to providing fundamental insights into the intimate link between premelting

and thermal stability at small length scales, our findings could be important in the design and understanding of stable nanoscale and cluster-based materials and devices.

ACKNOWLEDGMENTS

We acknowledge support from projects (No. FIS2008-02238, No. 2009SGR1041, and No. XRQTC) and computer time on *Marenostrum* (Barcelona Supercomputing Center). F.V. thanks the Spanish Ministerio de Ciencia e Innovación (MICINN) for a Juan de la Cierva grant (Grant No. JCI-2010-06372). J.C. is supported by MICINN by a Ramón y Cajal Fellowship. The authors gratefully acknowledge Professor Dr. Francesc Illas for fruitful discussions.

*Corresponding author: s.bromley@ub.edu

[1] J. W. M. Frenken and J. F. van der Veen, Phys. Rev. Lett. **54**, 134 (1985).
[2] A. M. Alseyad, M. F. Islam, J. Zhang, P. J. Collings, and A. G. Yodh, Science **309**, 1207 (2005).
[3] J. G. Dash, A. Rempel, and J. Wettlaufer, Rev. Mod. Phys. **78**, 695 (2005).
[4] M. Matsui and G. D. Price, Nature **351**, 735 (1991).
[5] H. Riegler and R. Köhler, Nat. Phys. **3**, 890 (2007).
[6] M. Schmidt, R. Kusche, B. V. Issendorff, and H. Haberland, Nature **393**, 238 (1998).
[7] F. Baletto and R. Ferrando, Rev. Mod. Phys. **77**, 371 (2005).
[8] A. Aguado and M. F. Jarrold, Annu. Rev. Phys. Chem. **62**, 151 (2011).
[9] H.-P. Cheng and R. S. Berry, Phys. Rev. A **45**, 7969 (1992).
[10] F. Calvo and F. Spiegelmann, Phys. Rev. Lett. **82**, 2270 (1999).
[11] J. Jellinek, T. L. Beck, and R. S. Berry, J. Chem. Phys. **84**, 2783 (1986).
[12] J. P. Rose and R. S. Berry, J. Chem. Phys. **98**, 3246 (1993).
[13] A. Heidenrich, I. Schek, D. Scharf, and J. Jortner, Z. Phys. D **20**, 227 (1991).
[14] T. Croteau and G. N. Patey, J. Chem. Phys. **124**, 244506 (2006).
[15] F. Calvo and P. Labastie, J. Phys. Chem. B **102**, 2051 (1998).
[16] P. C. R. Rodrigues and F. M. S. S. Fernandes, Int. J. Quant. Chem. **84**, 169 (2001).
[17] P. C. R. Rodrigues and F. M. S. S. Fernandes, Int. J. Quant. Chem. **110**, 284 (2010).
[18] J. P. Rose and R. S. Berry, J. Chem. Phys. **96**, 517 (1992).
[19] S. Sawada and S. Sugano, Z. Phys. D **12**, 189 (1989); **12**, 247 (1989).
[20] J. Jellinek, V. Bonačić-Koutecký, P. Fantucci, and M. Wiechert, J. Chem. Phys. **101**, 10092 (1994).
[21] A. A. Shvartsburg and M. F. Jarrold, Phys. Rev. Lett. **85**, 2530 (2000).
[22] S. Chacko, K. Joshi, and D. G. Kanhere, Phys. Rev. Lett. **92**, 135506 (2004).
[23] R. Pushpa, U. Waghmare, and S. Narasimhan, Phys. Rev. B **77**, 045427 (2008).
[24] J. M. Recio, R. Pandey, A. Ayuela, and A. B. Kunz, J. Chem. Phys. **98**, 4783 (1993).
[25] M.-J. Malliavin and C. Coudray, J. Chem. Phys. **106**, 2323 (1997).
[26] F. Bawa and I. Panas, Phys. Chem. Chem. Phys. **4**, 103 (2001).
[27] R. Dong, X. Chen, X. Wang, and W. Lu, J. Chem. Phys. **129**, 044705 (2008).
[28] W. A. Saunders, Phys. Rev. B **37**, 6583 (1988).
[29] P. J. Ziemann and A. W. Castleman, J. Chem. Phys. **94**, 718 (1991).
[30] J.-M. Leyssale and G. L. Vignoles, Chem. Phys. Lett. **454**, 299 (2008).
[31] S. C. Harvey, R. K.-Z. Tan, and T. E. Cheatman, J. Comput. Chem. **19**, 726 (1998).
[32] H.-S. Ahn, T.-E. Kim, E. Cho, M. Ji, C.-K. Lee, S. Han, Y. Cho, and C. Kim, J. Appl. Phys. **103**, 073518 (2008).
[33] L. Koči, R. Ahuja, A. B. Belonoshko, and B. Johansson, J. Phys.: Condens. Matter **19**, 016206 (2007).
[34] G. Kresse and J. Hafner, Phys. Rev. B **47**, 558 (1993).
[35] J. P. Perdew, J. A. Chevary, S. H. Vosko, K. A. Jackson, M. R. Pederson, D. J. Singh, and C. Fiolhais, Phys. Rev. B **46**, 6671 (1992); J. A. White and D. M. Bird, *ibid.* **50**, 4954 (1994).
[36] G. Kresse and D. Joubert, Phys. Rev. B **59**, 1758 (1999).
[37] G. Henkelman, B. P. Uberuaga, and H. Jonsson, J. Chem. Phys. **113**, 9901 (2000).
[38] A. Aguado and P. A. Madden, Phys. Rev. B **70**, 245103 (2004).
[39] Y. Zhang, H. S. Chen, B. X. Liu, C. R. Zhang, X. F. Li, and Y. C. Wang, J. Chem. Phys. **132**, 194304 (2010).
[40] D. Alfè, Phys. Rev. Lett. **94**, 235701 (2005).
[41] A. Aguado and P. A. Madden, Phys. Rev. Lett. **94**, 068501 (2005).
[42] K. Joshi, D. G. Kanhere, and S. A. Blundell, Phys. Rev. B **66**, 155329 (2002).
[43] R. Bader, Chem. Rev. **91**, 893 (1991).
[44] A. D. Becke and K. E. Edgecombe, J. Chem. Phys. **92**, 5397 (1990).
[45] H. Haberland, T. Hippler, J. Donges, O. Kostko, M. Schmidt, and B. von Issendorff, Phys. Rev. Lett. **94**, 035701 (2005).
[46] M. Schmidt, J. Donges, Th. Hippler, and H. Haberland, Phys. Rev. Lett. **90**, 103401 (2003).
[47] P. Chandrachud, K. Joshi, and D. G. Kanhere, Phys. Rev. B **76**, 235423 (2007).
[48] D. O. Welch, O. W. Lazareth, G. J. Dienes, and R. D. Hatcher, J. Chem. Phys. **68**, 2159 (1978).
[49] For the DF calculations of a charged cluster a homogeneous neutralizing background charge was employed to avoid spurious intercluster electrostatic interactions.
[50] K. Kwapien, M. Sierka, J. Döbler, J. Sauer, M. Haertelt, A. Fielicke, and G. Meijer, Angew. Chem. Int. Ed. **50**, 1716 (2011).